Check for updates

Optomechanically induced grating

MUQADDAR ABBAS,[1] **SEYYED HOSSEIN ASADPOUR,**[2] **HAMID R. HAMEDI,**[3] **AND ZIAUDDIN**[1,*]

[1]*Quantum Optics Lab. Department of Physics, COMSATS University Islamabad, Islamabad Campus 45550, Pakistan*
[2]*Department of Physics, Iran University of Science and Technology, Tehran, Iran*
[3]*Institute of Theoretical Physics and Astronomy, Vilnius University, Sauletekio, 3 LT-10257 Vilnius, Lithuania*
[*]ziauddin@comsats.edu.pk

Abstract: We suggest a flexible control of the diffraction grating by considering an optomechanical cavity system. The cavity is driven by an external control standing wave and realizes the characteristics of the diffraction grating when the light beam interacts with the cavity, a phenomenon which we name optomechanically induced grating (OMIG). A standing wave consists of nodes and antinodes that lead to gratings or slits in the cavity system. The reflected probe field from a moving mirror is diffracted through a standing wave and comes out through a partially reflected mirror. Effective control of the diffraction grating is achieved with the manipulation of the optomechanical strength g_{mc} (the so-called mirror-light interaction strength). Fascinatingly, the first, second, and third-order diffraction gratings can be easily achieved via the mirror-light interaction strength g_{mc}. The diffraction grating is found to be influenced by the cavity decay rate. For small values of the decay rate, the diffraction grating becomes maximum and vice versa. The results of our model can bring potential applications in optomechanical systems.

1. Introduction

Quantum interference and coherence are physical mechanisms which have recently lead to many interesting innovations in modern laser physics and quantum optics. One remarkable example of those fascinating innovations is the effect of electromagnetically induced transparency (EIT) which results in the elimination of the probe field absorption of an atomic medium at a resonance transition frequency [1–3]. The EIT plays an important role in quantum information science [4] and non-linear optics [5,6].

Interestingly, when a strong coupling field in an EIT scheme is replaced by a standing-wave (SW), the so called Electromagnetically Induced Grating (EIG) is observed. The probe field magnitude incident on an atomic grating changes in a periodic manner due to the spatial modulation formed by the SW field. The periodic modulation of the probe field results in the diffraction of light beam to higher orders just like classical grating. EIG was proposed first theoretically in 1998 [7]. It has been shown that the application of a strong SW control field interacting with a three-level atomic system diffracts a weak probe field into high-order diffractions. Following this theoretical representation of the EIG phenomenon, the experimental demonstration of EIG was also proposed in [8,9]. In another experiment, two counter-propagating fields with the same phase but propagating in the opposite directions have been employed to create an atomic grating within a medium [10]. Such a technique to generate EIG has certain applications in nonlinear optical processes, localizing the standing wave as well as for storage purposes in one-dimensional (1D), two-dimensional (2D) and three-dimensional (3D) optical pulses. Following this work, an experiment has been conducted to study the probe light transmission and reflection properties [11]. In the experiment [11], they observed EIG formation

in a vapor cell with a three-level atomic system which is dependent on laser frequency detunings. Using the propoerties of EIG, a method has been suggested for achieving all-optical routing and switching, which can be usefull in the quantum information process (QIP) and quantum networking [11]. EIG has drawn a lot of interest in different fields of science because of its possible applications such as all-optical switching and routing [11], switching of photonic band gaps [12], storage of light [10,13], beam splitting and fanning [14]. Different structures have been proposed theoretically to realize the EIG. For instance, a three-level ladder-type atom-light coupling scheme has been utilized to generate the EIG [15]. An enhanced diffraction grating has been observed by considering slightly off-resonant probe field detuning. It has been reported that for a four-level atomic structure, the atomic phase grating exhibits a giant Kerr nonlinearity [16].

On the other hand, optomechanics, which is at the core of quantum optics, explains the interaction between electromagnetic waves and nanomechanical motion. This form of interaction is more imperative at the micro and nanoscales, where the actual mass of the mechanical motion can be decreased substantially. Interaction of optical beams in the cavity with mechanically oscillating mirror via radiation pressure is known as cavity optomechanics [17,18]. Cavity optomechanics results in a variety of incredible further advances. Examples include, optomechanically induced transparency (OMIT) [19–25], precision measurements [26,27], quantum knowledge [28,29], modulation of light propagation [30,31], squeezing of light [32], and heavy coupling physics [33]. Note that, EIT [34], inverse EIT [35], Fano resonance [36,37], refractive index enhancement [38], and nano-scale optical cavities [22] have been already investigated. The multiple EIT can be obtained in atomic configurations by extending single EIT to different light-matter couplings, such as V-type [39], Y-type [40], N-type [41], and K-type [42] atomic media. Analogously, in charged optomechanical systems [43], coupled discs structures [44], coupled optomechanics [45], and double resonators optomechanics [46,47], a double OMIT window has been investigated.

A fascinating idea of nonlinearity can be introduced to an optomechanical cavity when it is excited by a strong field. This nonlinearity can be generated via the interaction between the mechanical mirror and the cavity field. This can lead to the manipulation of the refractive index of the cavity. It is now more interesting to study the manipulation of the diffraction grating in an optomechanical system instead of considering any medium. In the current article, we consider an optomechanical cavity and study the diffraction grating in the presence of a strong SW field. It is very exciting to show the dependence of the diffraction grating on the mirror-light interaction strength g_{mc} on the diffraction grating in an optomechanical cavity. Flexible control of the diffraction grating can be expected in the optomechanical cavity via mirror-light interaction strength g_{mc}. Our proposed model delivers an accessible technique to determine the optomechanical coupling strength by the amplification of diffraction grating that can be investigated in practical experiments.

2. Model

2.1. Dynamics of optomechanical cavity

We consider a hybrid optomechanical system, composed of a high Q Fabry-Perot cavity of length L, as shown in Fig. 1(a). The cavity is simultaneously driven by a standing wave (SW) beam of frequency ω_l and a weak probe field of frequency ω_p along the cavity axis. We also consider that both fields, the weak probe light beam and another position-dependent SW field interact with the cavity modes with the interaction length L. The energy-level diagram for an optomechanical system is shown in Fig. 1(b). The SW field pumps the cavity and couples the mechanical mode 3 to the cavity mode 2. The probe field couples the optical bath (1) to the cavity mode 2. In Fig. 1(c), the interaction of SW with the probe field is shown. The SW (nodes and antinodes) can be generated in the transverse (y) direction while the probe field is propagating in the longitudinal (x) direction. The Hamiltonian of the system can be expressed as [19]
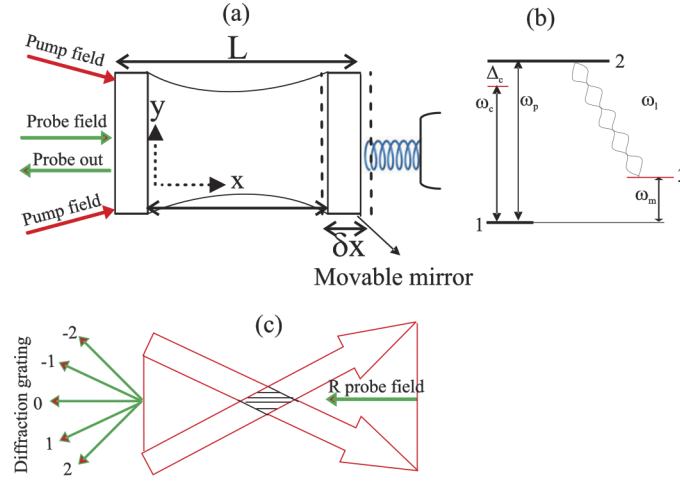
Fig. 1. (a) Schematic of the optomechanical cavity where two fields (probe and pump) are applied from the left to the cavity. (b) The energy-level configuration of the optomechanical cavity (c) Schematic of the diffraction grating when a probe field diffracts through a standing wave (like slits).

$$H = \hbar\Delta_c a^\dagger a + \left[\frac{p^2}{2m} + \frac{m\omega_m^2 x^2}{2}\right] - \hbar g_{mc} a^\dagger a x \qquad (1)$$
$$+ i\hbar\mathcal{E}_l(a^\dagger - a) + i\hbar(\mathcal{E}_p e^{-i\delta t}a^\dagger - \mathcal{E}_p^* e^{i\delta t}a),$$

where $\Delta_c = \omega_c - \omega_l$ represents the detuning of the cavity field frequency while $\delta = \omega_p - \omega_l$ denotes the difference in probe detuning and driving field. In Eq. (1) the first term shows the Hamiltonian for cavity mode with the creation ($a^\dagger$) and annihilation (a) operators. The second part of the Hamiltonian describes the unperturbed part for the moving mirror, where x and p are the position and momentum operators of vibrational mirror with the mass m and frequency ω_m. The parameter $g_{mc} = \frac{\omega_c}{L}\sqrt{\hbar/(2m\omega_m)}$ shows the coupling strength between the cavity and moving mirror. The last two parts of the Hamiltonian in Eq. (1) refer to the probe and control fields. The probe field amplitude is $|\mathcal{E}_p| = \sqrt{\frac{2\kappa P_p}{\hbar\omega_p}}$ and the pump field generates a SW field having frequency $\mathcal{E}_l = \mathcal{E}_m\sin[\pi y/\Lambda_y]$ whereas the pump field amplitude is $|\mathcal{E}_m| = \sqrt{\frac{2\kappa P_l}{\hbar\omega_l}}$. We use the Heisenberg equation of motion to explain the behavior of the optomechanical system. For a variable D, one can write the general equation as [48]

$$\frac{dD}{dt} = -\frac{i}{\hbar}[D, H] - \Gamma D + M, \qquad (2)$$

where Γ is the decay rate of a cavity photon and mechanical mirror whereas M accounts for the Brownian noise operator and input vacuum noise. After taking into account the corresponding fluctuation and dissipation terms and using Eq. (1), the Heisenberg equations of motion can be expressed as

$$\dot{x} = \frac{p}{m}, \qquad (3)$$

$$\dot{p} = -m\omega_m^2 x + \Gamma_m p + g_{mc}a^\dagger a + \zeta(t), \qquad (4)$$

$$\dot{a} = -(\kappa + i\Delta_c)a + ig_{mc}ax + \mathcal{E}_l + \mathcal{E}_p e^{-i\delta t} + \sqrt{2\kappa}a_{in}(t), \qquad (5)$$

where κ, is the cavity decay rate and Γ_m shows the decay rate of mechanical mode. It is also emphasized that the Langevin noise operator (Hermitian Brownian noise operator) affects

the system which have zero mean value $\langle \zeta(t) \rangle = 0$, and satisfies the temperature dependent correlation function $\langle \zeta(t) \zeta^\dagger(t') \rangle = \int \omega e^{-i\omega(t-t')} P(\omega) d\omega$. Here, $P(\omega) = \frac{\Gamma_m}{2\pi\omega_m}[1 + coth(\frac{\hbar\omega}{2k_BT})]$, k_B is the Boltzmann constant, and T is the temperature of the mechanical oscillator reservoir. We also incorporate the input vacuum noise into the cavity field $a_{in}(t)$ where the mean value of $a_{in}(t)$ goes to zero such as $\langle a_{in}(t) \rangle = 0$. In order to explain the effect of the mechanical cavity on the probe field transmission, we write the steady-state solutions of the corresponding operators which enables to study the output spectrum. Using the mean-field approximation [19], i.e., $\langle xa \rangle \approx \langle x \rangle \langle a \rangle$, the mean value equations read

$$\langle \dot{x} \rangle = \frac{\langle p \rangle}{m}, \tag{6}$$

$$\langle \dot{p} \rangle = -m\omega_m^2 \langle x \rangle - \Gamma_m \langle p \rangle + g_{mc} \langle c^\dagger \rangle \langle c \rangle, \tag{7}$$

$$\langle \dot{a} \rangle = -(\kappa + i\Delta_c)\langle a \rangle + ig_{mc}\langle a \rangle \langle x \rangle + \mathcal{E}_l + E_p e^{-i\delta t}. \tag{8}$$

Using the ansatz [49]

$$\langle x \rangle = x_s + x_- e^{-i\delta t} + x_+ e^{i\delta t} \tag{9}$$

$$\langle p \rangle = p_s + p_- e^{-i\delta t} + p_+ e^{i\delta t} \tag{10}$$

$$\langle a \rangle = a_s + a_- e^{-i\delta t} + a_+ e^{i\delta t}, \tag{11}$$

The steady state solution can be obtained as

$$a_s = \frac{\mathcal{E}_l}{\kappa + i(\Delta_c - \frac{g_{mc}}{\hbar} x_s)}, \tag{12}$$

where

$$x_s = \frac{\hbar g_{mc} |a|^2}{m\omega_m}.$$

Finally, the expression for a_- can be found in the following form

$$a_- = -\frac{A}{B}, \tag{13}$$

where

$$\begin{aligned} A = &-im\Gamma_m\delta^2\hbar - m\delta^3\hbar + m\Gamma_m\delta\kappa\hbar - im\delta^2\kappa\hbar \\ &+ m\delta\omega_m^2\hbar + im\kappa\omega_m^2\hbar - im\gamma\delta\Delta_c\hbar - m\delta^2\Delta_c\hbar \\ &+ m\omega_m^2\Delta_c\hbar - |a_s|^2 g_{mc}^2, \end{aligned}$$

and

$$\begin{aligned} B = &(m\Gamma_m\delta^3\hbar - im\delta^4\hbar + 2im\Gamma_m\delta^2\kappa\hbar + 2m\delta^3\kappa\hbar \\ &-m\Gamma_m\delta\kappa^2\hbar + im\delta^2\kappa^2\hbar + im\delta^2\omega_m^2\hbar - 2m\delta\kappa\omega^2\hbar \\ &-im\kappa^2\omega^2\hbar - im\kappa^2\omega_m^2\hbar - m\Gamma_m\delta\Delta_c^2\hbar + im\delta^2\Delta_c^2\hbar \\ &-im\omega_m^2\Delta_c^2\hbar + 2ig_{mc}^2\Delta_c |a_s|^2). \end{aligned}$$

One may write the input-output relation of the cavity as [50]

$$E_{out}(t) + \mathcal{E}_p e^{-i\delta t} + \mathcal{E}_l = \sqrt{2\kappa}a, \tag{14}$$

where

$$E_{out}(t) = E_{out}^0 + E_{out}^+ \mathcal{E}_p e^{-i\delta t} + E_{out}^- \mathcal{E}_p e^{i\delta t}. \tag{15}$$

Solving Eqs. (14) and (15), one gets

$$E_{out}^+ = \frac{\sqrt{2\kappa}a_-}{\mathcal{E}_p} - 1,$$ (16)

which can be measured by using the homodyne technique [50]. For convenience, we define

$$E_{out}^+ + 1 = \frac{\sqrt{2\kappa}a_-}{\mathcal{E}_p} = \mathcal{E}_T.$$ (17)

The quadratures of the field $\mathcal{E}_T$ can be defined as $\mathcal{E}_T = Re[\mathcal{E}_T] + iIm[\mathcal{E}_T]$. Here, $Re[\mathcal{E}_T]$ and $Im[\mathcal{E}_T]$ are the out-of-phase and in-phase quadratures of the output probe field, respectively.

The phenomenon of OMIT has been previously studied [19–25] which depends on the phase dispersion in the OMIT window. The phase dispersion of the output probe field can be expressed as

$$\phi_1(\omega_p) = \arg[t_p(\omega_p)],$$ (18)

where $t_p(\omega_p)$ is the probe field transmission and can be defined as

$$t_p(\omega_p) = 1 - \frac{\sqrt{2\kappa}a_-}{\mathcal{E}_p}.$$ (19)

2.2. Dynamics of OMIG

Using the Maxwell's equation, one arrives at the following equation for the propagation of probe light beam (E_p) [7]

$$\frac{\partial E_p}{\partial x} = [\alpha(y) + i\beta(y)]E_p,$$ (20)

where $\alpha(y) = (\frac{2\pi}{\lambda})Re[\mathcal{E}_T]$ and $\beta(y) = (\frac{2\pi}{\lambda})Im[\mathcal{E}_T]$ are the absorption and dispersion coefficients of the probe field having wavelength λ, respectively.

For simplification, we focus on the characteristics of the OMIG by ignoring the transverse part in Eq. (20) [7]. The transmission function of the probe light beam at $y = L$ can be easily calculated using Eq. (20), yielding

$$T(y) = e^{-\alpha(y)L + i\beta(y)L},$$ (21)

where the terms $|T(y)| = e^{\alpha(y)L}$ and $\phi_2(y) = \beta(y)L$ are associated with the amplitude and phase modulation of the cavity, respectively. Assuming that the input probe field is a plane wave, the diffraction intensity distribution can be expressed as [7,51,52]

$$I(\theta) = |E(\theta)|^2 \times \frac{\sin^2(N\pi\Lambda_y \sin(\theta)/\lambda)}{N^2 \sin^2(\pi\Lambda_y \sin(\theta)/\lambda)},$$ (22)

where N is the number of spatial periods of optomechanically induced grating, θ stands for the diffraction angle along the y-direction, and the parameter $\Lambda_y = \frac{\pi}{k_y}$ denotes the spatial period in the y direction, whereas the term $E(\theta)$ is the Fourier transform of $T(y)$ and describes the Fraunhofer diffraction for a single period as

$$E(\theta) = \int_0^1 T(y)e^{-2\pi i\Lambda_y y \sin(\theta)/\lambda}dy.$$ (23)

3. Results and discussion

To start the discussion first we show the behavior of the output probe field in the absence and the presence of mirror-light interaction strength g_{mc}. We display in Fig. 2(a) the spectrum of OMIT (Re[$\mathcal{E}_T$]) versus the normalized δ/ω_m for different values of g_{mc}. In the absence of g_{mc}, we find a Lorentzian shape with high absorption of the probe field in the cavity, as shown by the solid green curve. In the presence of a small value of $g_{mc}/2\pi = 0.4$MHz, there is a hole bored into the spectrum of the output probe field as illustrated by the dashed blue curve, resulting in a narrow transparency window. The larger the value of g_{mc}, the broader the transparency window, see the dotted red curve in Fig. 2(a). We also depict in Fig. 2(b) the phase ($\phi_1(\omega_p)$) of the output probe field representing the dispersive properties of the optomechanical cavity for certain values of g_{mc}. The slope may alter with changing the value of g_{mc} as shown by dashed blue and dotted red curves. In particular, for $g_{mc} = 0$, the slope is negative corresponding to a negative group index of the cavity. For non-zero values of g_{mc}, the slope changes to positive, suggesting the slow light condition.
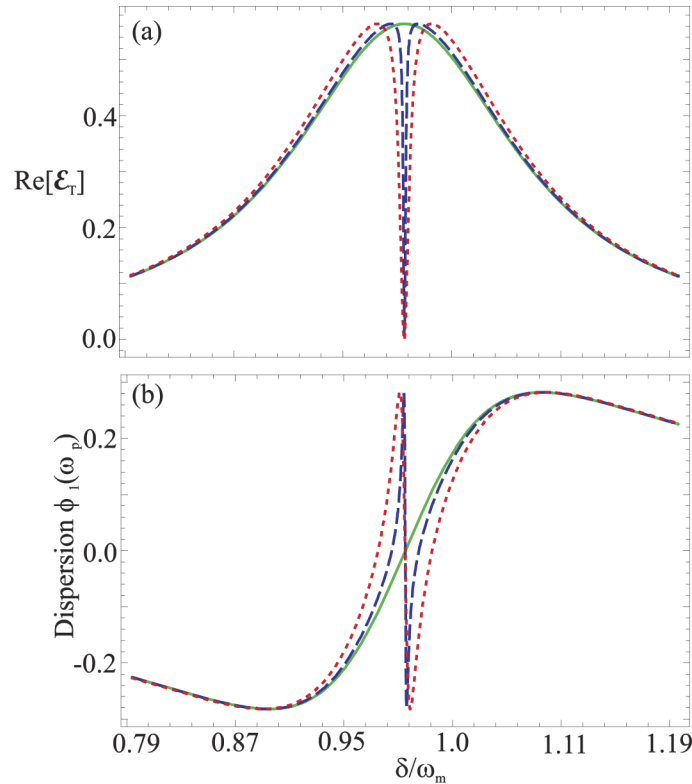

Fig. 2. (a) The real part of $\mathcal{E}_{out}$ (absorption) versus δ/ω_m. (b) The phase $\phi_1(\omega_p)$ versus δ/ω_m. The solid green curve is shown for $g_{mc} = 0$, the dotted-dashed blue curve is for $g_{mc}/2\pi = 0.4$MHz and dashed red curve is for $g_{mc}/2\pi = 1$MHz. The parameters are, $\mathcal{E}_m/2\pi = 1$MHz, $\omega_m/2\pi = 10$MHz, $\kappa = \omega_m/10$, $\Delta_c/2\pi = 10$MHz, and $\Gamma_m/2\pi = 140$Hz

Before discussing the grating, it is necessary to discuss the amplitude $T(y)$ and phase $\phi_2(y)$ modulation of the transmission functions. In Fig. 3 we plot $T(y)$ and $\phi_2(y)$ versus y for different values of mirror-light interaction strength g_{mc}. We get nodes and antinodes in the period while the antinodes increase with increasing the value of g_{mc} as can be seen in Fig. 3(a). When $g_{mc} = 0$, $|Ty|$ approaches to zero as shown by the solid red curve in Fig. 3(a). It means that when the pump

field is zero then gmc = 0, this shows that all the probe light will be absorbed in the cavity system. The transmission of probe light becomes zero when there is high absorption in the cavity system. It is now difficult to realize the diffraction grating for $g_{mc} = 0$. It is obvious that by increasing the mirror-light interaction strength, the probe field enhances while it depends on the transverse coordinate y. For the non-zero values of g_{mc}, we find that the amplitude becomes maximum for higher values. Similarly, we show in Fig. 3(b) the phase modulation of the transmission function for different values of g_{mc}. It is seen that the phase modulation is also dependent on the mirror-light interaction strength and can be modified with changing the value of g_{mc}.
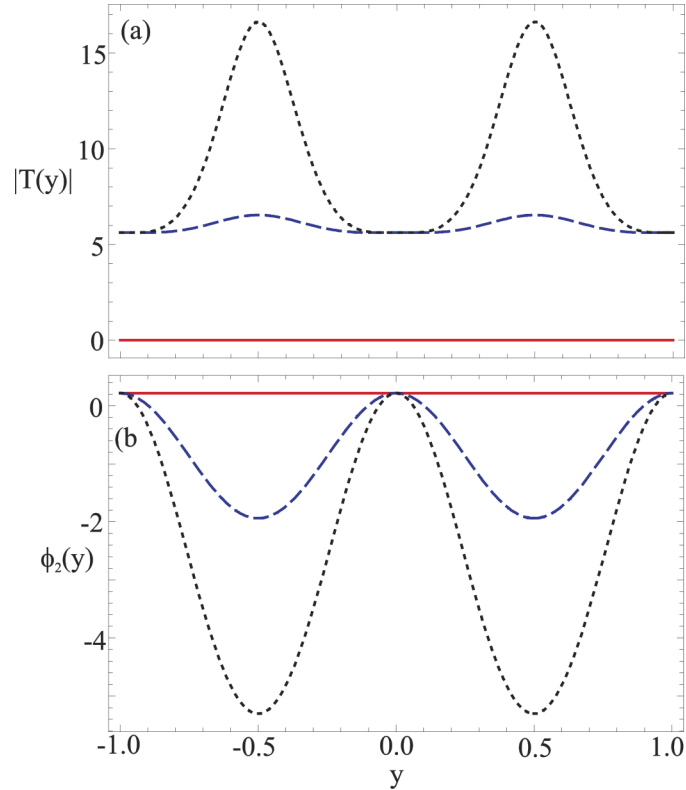

Fig. 3. (a) The Amplitude $|T|$ and (b) phase $\phi_2(y)$ of the transmission versus y. The solid red curve is shown for $g_{mc}/2\pi = 0$, the dashed blue curve is shown for $g_{mc}/2\pi = 0.4$MHz and dotted black curve is shown for $g_{mc}/2\pi = 0.5$MHz. The parameters are, $\mathcal{E}_m/2\pi = 0.5$MHz, $\omega_m/2\pi = 10$MHz, $\kappa = \omega_m/10$, $\Delta_c/2\pi = 10$MHz, $\delta/2\pi = 10$MHz, and $\Gamma_m/2\pi = 140$Hz

As noted, the diffraction grating in ordinary media such as in atomic systems has been explored earlier (the EIG effect) [15,16]. On the other hand, the concept of OMIT has been widely studied by utilizing different techniques [19–25]. In what follows, we develop the theory to realize the diffraction grating through the optomechanical cavity by combining the EIG and OMIT effects. We consider a simple optomechanical cavity and characterize the OMIG in the presence of a strong SW field by simply tuning the knob of the mirror-light interaction strength g_{mc}. To study the OMIG, we use Eq. (22) and plot first the intensity of diffraction grating distribution as a function of $\sin\theta$ for the case that the mirror-light interaction strength g_{mc} is absent (see Fig. 4(a)). One can observe no OMIG in the spectrum for $g_{mc} = 0$. This is the case for which no OMIT occurs in the system, as all the probe light is absorbed in the absence of g_{mc}. It is emphysized that the SW field interacts with the movable mirror and can generate the radiation pressure inside the cavity. The generation of radiation pressure inside the cavity leads to generate the mirror-light

interaction strength g_{mc}. It means that g_{mc} is dependent on the SW field in the cavity system. Therefore, no OMIG can be observed when $g_{mc} = 0$ and vice versa. Further, the nodes and antinodes or slits can only be generated when SW field is switch on and in this situation the value of $g_{mc} \neq 0$.
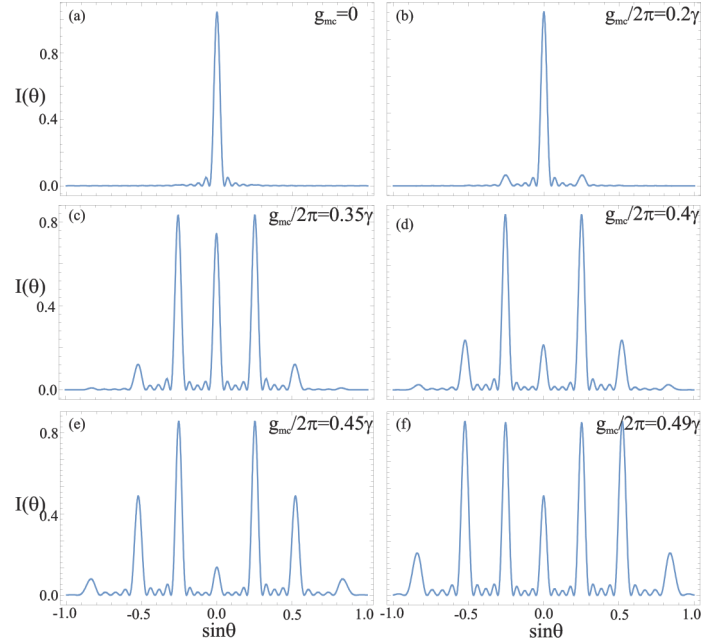

Fig. 4. The diffraction intensity distribution $I(\theta)$ versus $\sin\theta$ for different values of g_{mc} (a) $g_{mc} = 0$ (b) $g_{mc}/2\pi = 0.2$MHz (c) $g_{mc}/2\pi = 0.35$MHz (d) $g_{mc}/2\pi = 0.4$MHz,(e) $g_{mc}/2\pi = 0.45$MHz and (f) $g_{mc}/2\pi = 0.49$MHz . The other parameters are $\mathcal{E}_m/2\pi = 0.5$MHz, $\omega_m/2\pi = 10$MHz, $\kappa = \omega_m/10$, $N = 5$, $L = 50\mu m$, $\Lambda_y = 4\lambda$, $\Delta_c/2\pi = 10$MHz, $\delta/2\pi = 10$MHz, and $\Gamma_m/2\pi = 140$Hz

As shown in Fig. 2(a), the OMIT can be only achieved when $g_{mc} \neq 0$. Let us next consider a situation where the mirror-light interaction strength plays a role i.e., $g_{mc} \neq 0$, and study thoroughly the behaviors of OMIG for different values of g_{mc}. Setting $g_{mc}/2\pi = 0.2$MHz, the first order OMIG is generated as illustrated in Fig. 4(b), with a little energy being transferred to the first order. For further increment in $g_{mc}/2\pi$ from 0.2MHz to 0.35MHz, the first-order diffraction increases along with the generation of second-order diffraction grating, as can be observed in Fig. 4(c). Interestingly, the maximum energy of the probe field transfers to the first-order of diffraction grating, see Figs. 4(c, d, e). It will be more interesting to transfer the probe energy to the second-order diffraction grating. To get this, we set $g_{mc}/2\pi = 0.49$MHz and plot $I(\theta)$ versus $\sin\theta$, see Fig. 4(f). It is clearly demonstrated that the probe energy transfers to the first and second-order diffraction gratings. One can also see from Fig. 4(f) that the energy of the probe field is also transferred to the third-order diffraction which is very constructive. It is now clear that the optomechanical cavity system diffracts the probe light into different directions and also enhances the amplitude of probe light, indicating that our model acts as a phase and amplitude grating. The physical picture of the diffraction grating in our optomechanical system is presented in Fig. 1(c). The external control and a weak probe fields are applied from left to the cavity system and exert pressure on the movable mirror. A SW is generated in the cavity that consists of nodes and antinodes that leads to gratings in the system. The probe field is reflected from the

movable mirror and interact with the gratings that can be diffracted in different directions. In this way diffraction grating is generated in our proposed system.

A 3D plot of the diffraction intensity distribution spectra versus $\sin\theta$ and g_{mc} can provide a better perspective of this phenomenon, as shown in Fig. 5. For very small values of g_{mc} ($g_{mc} \rightarrow 0$), the central intensity (the zeroth order) is maximum and no grating takes place in different directions. The probe energy starts to transfer to the first-order when $g_{mc}/2\pi \approx 0.2$MHz. For larger values of g_{mc}, the probe energy increases in first-order while little energy is being also transferred to the second-order. When $g_{mc}/2\pi \approx 0.45$MHz, the probe energy can be transferred to the first, second and third-orders, while the central intensity goes to zero.
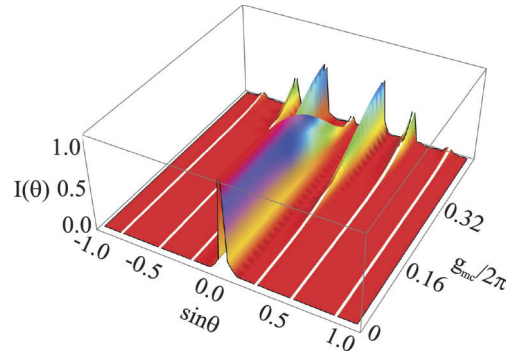

Fig. 5. The 3D plot of diffraction intensity distribution $I(\theta)$ versus $\sin\theta$ and $g_{mc}/2\pi$. The parameters are $g_{mc}/2\pi = 0.49$MHz, $\mathcal{E}_m/2\pi = 0.5$MHz, $\omega_m/2\pi = 10$MHz, $\kappa = \omega_m/10$, $N = 5$, $L = 50\mu m$, $\Lambda_y = 4\lambda$, $\Delta_c/2\pi = 10$MHz, $\delta/2\pi = 10$MHz and $\Gamma_m/2\pi = 140$Hz

To elucidate better the influence of g_{mc} on the first, second, and third-order diffraction gratings separately, we display them in Fig. 6 for different diffracted angles. For the first-order diffraction grating (dashed blue curve), we take $\theta = 0.25$ radian and plot it versus g_{mc} for $\delta/\omega_m = 10$MHz. The probe energy is seen to transfer to the first-order while increases with increasing the value of g_{mc}. For the same parameters but $\theta = 0.52$ radian and 0.84 radian, the second (dotted red curve) and third-order (solid green curve) diffraction gratings are shown versus g_{mc}, respectively. It is apparent that the second and third-order diffraction gratings are also increasing by increasing the value of g_{mc}. One notices that the maximum probe energy transfers to the first-order diffracting grating while little energy is sent to the third-order, with an intermediate transfer to the second-order of diffraction grating. The inset in Fig. 6 shows the variation of diffraction grating versus g_{mc} for small ranges.

The optomechanical cavity is a lossy system as one of its mirrors is partially reflecting. The pump and probe fields propagate in and become out of the cavity. Consequently, the photons of the cavity have a limited lifetime and decay at a rate known as the decay rate of the cavity (κ). The decay rate of the cavity depends upon the Q-factor of the cavity. The cavity decay rate follows $\kappa \propto 1/\tau_c$, where τ_c is the lifetime of the cavity photons. Therefore, the decay rate κ may affect the output probe field. The change in the output probe field then leads to manipulating the OMIT, and this results in the diffraction grating in the optomechanical system (when applying a control SW field). In the following, we study the influence of κ on the diffraction grating when $\delta/\omega_m = 10$MHz. A 3D plot of the intensity distribution versus $\sin\theta$ and κ/ω_m is shown in Fig. 7. The diffraction grating is zero (or very close to zero) for larger values of κ/ω_m. This means that there will be no diffraction if the cavity decays very strong. The diffraction grating enhances with the decrease of cavity decay κ/ω_m as shown in Fig. 7.

The decay rate of the mechanical mode can also influence the behavior of the output probe field. The absorption in the optomechanical cavity increases with increasing the decay rate of
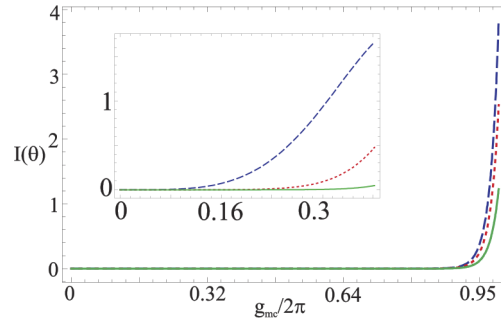
Fig. 6. The first (blue dashed for $\theta = 0.25$ radian), second (red dotted for $\theta = 0.52$ radian) and third-order (solid green for $\theta = 0.84$ radian) diffraction intensity distribution $I(\theta)$ versus $g_{mc}/2\pi$. The other parameters are $g_{mc}/2\pi = 0.49$MHz, $\mathcal{E}_m/2\pi = 0.5$MHz, $\omega_m/2\pi = 10$MHz, $N = 5$, $L = 50\mu m$, $\Lambda_y = 4\lambda$, $\Delta_c/2\pi = 10$MHz, $\delta/2\pi = 10$MHz and $\Gamma_m/2\pi = 140$Hz
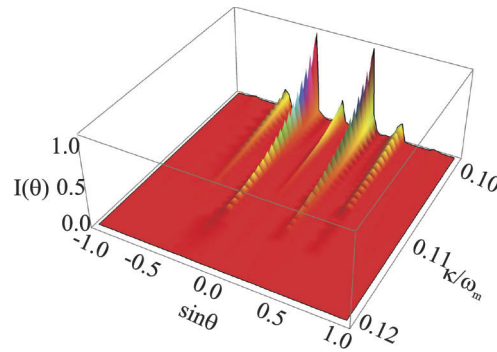

Fig. 7. The 3D plot of diffraction intensity distribution $I(\theta)$ versus $sin\theta$ and κ/ω_m. The other parameters are $g_{mc}/2\pi = 0.49$MHz, $\mathcal{E}_m/2\pi = 0.5$MHz, $\omega_m/2\pi = 10$MHz, $N = 5$, $L = 50\mu m$, $\Lambda_y = 4\lambda$, $\Delta_c/2\pi = 10$MHz, $\delta/2\pi = 10$MHz and $\Gamma_m/2\pi = 140$Hz

mechanical mode Γ_m. The absorption in the system can influence the diffraction grating in the system. Now it will be more attractive to study the influence of the decay rate of mechanical mode Γ_m on the OMIG. We consider two values of Γ_m and plot the diffraction intensity distribution versus $sin\theta$ as depicted in Fig. 8. The first, second, and third orders diffraction grating reduces by considering a large value of Γ_m such as $\Gamma_m/2\pi = 14$kHz, see Fig. 8(a). The diffraction grating disappears when a large value such as $\Gamma_m/2\pi = 140$kHz is considered as shown in Fig. 8(b).

3.1. *Experimental realization of OMIG*

The possible experimental realization of the proposed model is presented. The potential dimension of the optomechanical cavity system can be in the order of micrometers [33]. The experimental realization of OMIT in an optomechanical cavity system has been reported [20,24]. Similarly, the strong coupling of a micromechanical cavity with an optical cavity has also been revealed experimentally [33]. Our proposed system is based on the experimental realization [20,24,33]. In the experiments [20,24,33], the intensity of the output probe field is recorded for the observation of OMIT. Now the nodes and antinodes can be generated in the optomechanical system by considering the strong pump field is a SW field. Here, the nodes block the probe field where the antinodes scatter the probe field. The scattered intensity can be recorded on the screen and one can get the diffraction grating. In our theoretical study, we used the experimental setup and possible
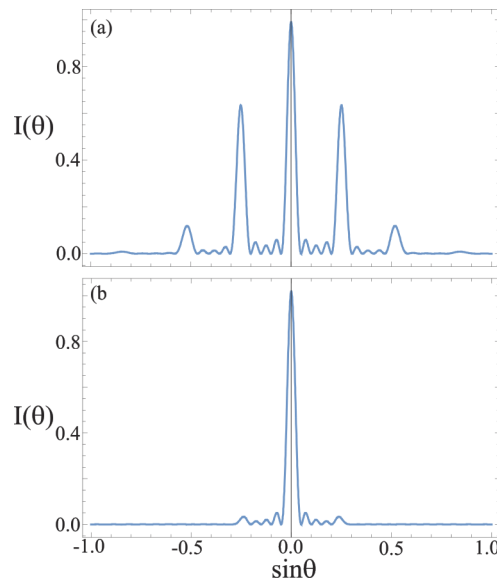
Fig. 8. The diffraction intensity distribution $I(\theta)$ versus $\sin\theta$ for different values of Γ_m (a) $\Gamma_m/2\pi = 14$kHz (b) $\Gamma_m/2\pi = 140$kHz . The other parameters are $\mathcal{E}_m/2\pi = 0.5$MHz, $\omega_m/2\pi = 10$MHz, $\kappa = \omega_m/10$, $N = 5$, $L = 50\mu m$, $\Lambda_y = 4\lambda$, $\Delta_c/2\pi = 10$MHz, $\delta/2\pi = 10$MHz.

experimental parameters [33]. In Ref. [33], the mechanical frequency is set to $\omega_m \approx 1$MHz. However, it is also mentioned in this reference that the typical mechanical frequency could be $\omega_m = 10$MHz indicating that in an experiment, one may consider the mechanical frequency in the range from 1 MHz to 10 MHz. Therefore, we safely conclude that the phenomenon of OMIG can be observed experimentally in our proposed optomechanical cavity in the future.

4. Summary

We have theoretically studied the OMIG effect in an optomechanical cavity system. An external control field is considered as a standing wave, enabling to realize the characteristics of the diffraction grating via the mirror-light interaction strength g_{mc}. It has been demonstrated that the first, second and third-order diffraction gratings are all possible to achieve by tuning the mirror-light interaction strength. We have shown that the decay rate of the cavity also affects the diffraction grating patterns. In particular, one obtains a maximum OMIG for small values of the decay rate. Our model paves the way toward further theoretical and experimental studies to explore the OMIG as well as new stimulating phenomena in optomechanical cavity systems.

Disclosures. The authors declare no conflicts of interest.

Data availability. Data underlying the results presented in this paper are not publicly available at this time but may be obtained from the authors upon reasonable request.

References

1. M. O. Scully and M. S. Zubairy, "Quantum Optics," (Cambridge University Press, England, 1997).
2. S. E. Harris, "Electromagnetically Induced Transparency," Phys. Today **50**(7), 36–42 (1997).
3. M. Fleischhauer, A. Imamoglu, and J. P. Marangos, "Electromagnetically induced transparency: Optics in coherent media," Rev. Mod. Phys. **77**(2), 633–673 (2005).
4. M. D. Lukin and A. Imamoglu, "Controlling photons using electromagnetically induced transparency," Nature (London) **413**(6853), 273–276 (2001).
5. M. D. Lukin and A. Imamoglu, "Nonlinear Optics and Quantum Entanglement of Ultraslow Single Photons," Phys. Rev. Lett. **84**(7), 1419–1422 (2000).

6. M. Yan, E. G. Rickey, and Y. F. Zhu, "Nonlinear absorption by quantum interference in cold atoms," Opt. Lett. **26**(8), 548 (2001).
7. H. Y. Ling, Y. -Q. Li, and M. Xiao, "Electromagnetically induced grating: Homogeneously broadened medium," Phys. Rev. A **57**(2), 1338–1344 (1998).
8. M. Mitsunaga and N. Imoto, "Observation of an electromagnetically induced grating in cold sodium atoms," Phys. Rev. A **59**(6), 4773–4776 (1999).
9. G. C. Cardoso and J. W. R. Tabosa, "Electromagnetically induced gratings in a degenerate open two-level system," Phys. Rev. A **65**(3), 033803 (2002).
10. M. Bajcsy, A. S. Zibrov, and M. D. Lukin, "Stationary pulses of light in an atomic medium," Nature (London) **426**(6967), 638–641 (2003).
11. A. W. Brown and M. Xiao, "All-optical switching and routing based on an electromagnetically induced absorption grating," Opt. Lett. **30**(7), 699 (2005).
12. S. -q. Kuang, R. -g. Wan, J. Kou, Y. Jiang, and J. -y. Gao, "Tunable double photonic bandgaps in a homogeneous atomic medium," J. Opt. Soc. Am. B **27**(8), 1518 (2010).
13. D. Moretti, D. Felinto, J. W. R. Tabosa, and A. Lezama, "Dynamics of a stored Zeeman coherence grating in an external magnetic field," J. Phys. B **43**(11), 115502 (2010).
14. L. Zhao, W. Duan, and S. F. Yelin, "All-optical beam control with high speed using image-induced blazed gratings in coherent media," Phys. Rev. A **82**(1), 013809 (2010).
15. B. K. Dutta and P. K. Mahapatra, "Electromagnetically induced grating in a three-level Lambda-type system driven by a strong standing wave pump and weak probe fields," J. Phys. B **39**(5), 1145–1157 (2006).
16. L. E. E. de Araujo, "Electromagnetically induced phase grating," Opt. Lett. **35**(7), 977 (2010).
17. T. J. Kippenber and J. K. Vahala, "Cavity Opto-Mechanics," Opt. Express **15**(25), 17172 (2007).
18. M. Aspelmeyer, T. J. Kippenberg, and F. Marquardt, "Cavity optomechanics," Rev. Mod. Phys. **86**(4), 1391–1452 (2014).
19. G. S. Agarwal and S. Huang, "Electromagnetically induced transparency in mechanical effects of light," Phys. Rev. A **81**(4), 041803 (2010).
20. S. Weis, R. Riviére, S. Deléglise, E. Gavartin, O. Arcizet, A. Schliesser, and T. J. Kippenberg, "Optomechanically Induced Transparency," Science **330**(6010), 1520–1523 (2010).
21. J. B. Khurgin, M. W. Pruessner, T. H. Stievater, and W. S. Rabinovich, "Laser-Rate-Equation Description of Optomechanical Oscillators," Phys. Rev. Lett. **108**(22), 223904 (2012).
22. E. Verhagen, S. Deleglise, S. Weis, A. Schliesser, and T. J. Kippenberg, "Quantum-coherent coupling of a mechanical oscillator to an optical cavity mode," Nature **482**(7383), 63–67 (2012).
23. H. Xiong, L. G. Si, A. S. Zheng, X. Yang, and Y. Wu, "Higher-order sidebands in optomechanically induced transparency," Phys. Rev. A **86**(1), 013815 (2012).
24. M. Karuza, C. Biancofiore, C. Molinelli, M. Galassi, R. Natali, P. Tombesi, G. D. Giuseppe, and D. Vitali, "Optomechanically induced transparency in a membrane-in-the-middle setup at room temperature," Phys. Rev. A **88**(1), 013804 (2013).
25. D. E. Chang, A. H. Safavi-Naeini, M. Hafezi, and O. Painter, "Slowing and stopping light using an optomechanical crystal array," New J. Phys. **13**(2), 023003 (2011).
26. J. Q. Zhang, Y. Li, M. Feng, and Y. Xu, "Precision measurement of electrical charge with optomechanically induced transparency," Phys. Rev. A **86**(5), 053806 (2012).
27. Q. Wang, J. Q. Zhang, P. C. Ma, C. M. Yao, and M. Feng, "Precision measurement of the environmental temperature by tunable double optomechanically induced transparency with a squeezed field," Phys. Rev. A **91**(6), 063827 (2015).
28. K. Stannigel, P. Komar, S. J. M. Habraken, S. D. Bennett, M. D. Lukin, P. Zoller, and P. Rabl, "Optomechanical Quantum Information Processing with Photons and Phonons," Phys. Rev. Lett. **109**(1), 013603 (2012).
29. P. Kómár, S. D. Bennett, K. Stannigel, S. J. M. Habraken, P. Rabl, P. Zoller, and M. D. Lukin, "Single-photon nonlinearities in two-mode optomechanics," Phys. Rev. A **87**(1), 013839 (2013).
30. H. Xiong, L. G. Si, and Y. Wu, "Precision measurement of electrical charges in an optomechanical system beyond linearized dynamics," Appl. Phys. Lett. **107**(9), 091116 (2015).
31. H. Xiong, C. Yang, X. Yang, and Y. Wu, "Optical polarizer based on the mechanical effect of light," Opt. Lett. **41**(18), 4316 (2016).
32. T. P. Purdy, P.-L. Yu, R. W. Peterson, N. S. Kampel, and C. A. Regal, "Strong Optomechanical Squeezing of Light," Phys. Rev. X **3**(3), 031012 (2013).
33. S. Gröblacher, K. Hammerer, M. R. Vanner, and M. Aspelmeyer, "Observation of strong coupling between a micromechanical resonator and an optical cavity field," Nature **460**(7256), 724–727 (2009).
34. S. E. Harris, J. E. Field, and A. Imamoglu, "Nonlinear optical processes using electromagnetically induced transparency," Phys. Rev. Lett. **64**(10), 1107–1110 (1990).
35. G. S. Agarwal and S. Huang, "Nanomechanical inverse electromagnetically induced transparency and confinement of light in normal modes," New J. Phys. **16**(3), 033023 (2014).
36. U. Fano, "Effects of Configuration Interaction on Intensities and Phase Shifts," Phys. Rev. **124**(6), 1866–1878 (1961).
37. C. Ott, A. Kaldun, P. Raith, K. Meyer, M. Laux, J. H. Evers, C. Keitel, C. H. Greene, and T. Pfeifer, "Lorentz Meets Fano in Spectral Line Shapes: A Universal Phase and Its Laser Control," Science **340**(6133), 716–720 (2013).

38. L. Zhang and J. Evers, "Uniform phase modulation via control of refractive index in a thermal atom vapor with vanishing diffraction or absorption," Phys. Rev. A **90**(2), 023826 (2014).

39. K. Ying, Y. Niu, D. Chen, H. Cai, R. Qu, and S. Gong, "Observation of Multi-Electromagnetically Induced Transparency in V-type Rubidium Atoms," J. Mod. Opt. **61**(8), 631–635 (2014).

40. L. Safari, D. Iablonskyi, and F. Fratini, "Double-Electromagnetically Induced Transparency in a Y-type atomic system," Eur. Phys. J. D **68**(2), 27 (2014).

41. Y. Chen, X. G. Wei, and B. S. Ham, "Optical properties of an N-type system in Doppler-broadened multilevel atomic media of the rubidium D_2 line," J. Phys. B **42**(6), 065506 (2009).

42. B. P. Hou, S. J. Wang, W. L. Yu, and W. L. Sun, "Double electromagnetically induced two-photon transparency in a five-level atomic system," Phys. Lett. A **352**(4-5), 462–466 (2006).

43. P. C. Ma, J. Q. Zhang, Y. Xiao, M. Feng, and Z. M. Zhang, "Tunable double optomechanically induced transparency in an optomechanical system," Phys. Rev. A **90**(4), 043825 (2014).

44. S. Jing, "Electromagnetically Induced Transparency in an Optomechanical System," Chin. Phys. Lett. **28**(10), 104203 (2011).

45. W. J. Gu and Z. Yi, "Double optomechanically induced transparency in coupled-resonator system," Opt. Commun. **333**, 261–264 (2014).

46. S. Shahidani, M. H. Naderi, and M. Soltanolkotabi, "Control and manipulation of electromagnetically induced transparency in a nonlinear optomechanical system with two movable mirrors," Phys. Rev. A **88**(5), 053813 (2013).

47. Mujeeb-ur-Rahman Ziauddin, "Control of slow-to-fast light and single-to-double optomechanically induced transparency in a compound resonator system: A theoretical approach," Europhys. Lett. **120**(2), 24001 (2017).

48. V. Giovannetti and D. Vitali, "Phase-noise measurement in a cavity with a movable mirror undergoing quantum Brownian motion," Phys. Rev. A **63**(2), 023812 (2001).

49. R. W. Boyd, *Nonlinear Optics* (Academic, New York, 2010).

50. D. F. Walls and G. J. Milburn, "Quantum Optics," Springer-Verlag, Berlin/Heideberg 127, (2007).

51. S. Q. Kuang, C. S. Jin, and C. Li, "Gain-phase grating based on spatial modulation of active Raman gain in cold atoms," Phys. Rev. A **84**(3), 033831 (2011).

52. E. Hecht and A. R. Ganesan, "Optics," 4th edition Perarson (2008).